This is an open access article published under an ACS AuthorChoice License, which permits copying and redistribution of the article or any adaptations for non-commercial purposes.

ACS OMEGA

Article

Cite This: ACS Omega 2019, 4, 21230−21241

http://pubs.acs.org/journal/acsodf

Parameter Estimation and an Extended Predictive-Based Tuning Method for a Lab-Scale Distillation Column

Eadala Sarath Yadav,[†] Thirunavukkarasu Indiran,*[,†] S. Shanmuga Priya,[‡] and Giuseppe Fedele[§]

[†]Department of Instrumentation and Control Engineering and [‡]Department of Chemical Engineering, Manipal Institute of Technology, Manipal Academy of Higher Education, 576104 Manipal, Karnataka, India

[§]Department of Informatics, Modeling, Electronics and Systems Engineering, University of Calabria, 87036 Rende (CS), Italy

ABSTRACT: The present study proposes a new PI controller tuning method using extended predictive control (EPC). The PI controller parameter values are calculated using the EPC controller output and its closed-loop response. This provides a simple and an effective tuning strategy which results in an improved closed-loop response compared to conventional tuning methods. The tuning methodology is applicable for single input single output and multi input multi output stable processes. Simulation and experimental results reveal the efficacy of the method under plant uncertainty conditions.

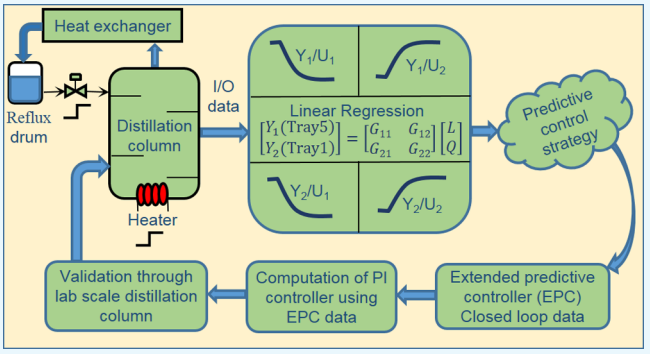

1. INTRODUCTION

The three term control (PID) has been one of the simplest and most popular control approaches over six decades. The major demand of PID is due to its simple structure, ease of use, and robustness.[1] Apart from a conventional structure, the control loops are modified in many ways in order to obtain better performance and efficiency.[2,3] The drawback of the traditional PID controller is that it cannot handle constraints, it cannot manage strong interactions, and it is generally used in the control of simple processes.[4] Therefore, off-the-shelf algorithms are not an optimal choice in many processes.[5] This limitation has extended research toward advanced control areas like optimal, robust, and adaptive control.[6−8] The recent developments comprise event-triggered control that deals with the problems of finite communication for constrained nonlinear systems through optimal policy.[9] Model predictive control (MPC) is another control approach, which is able to handle the process interactions and constraints. It is a popular and widely used control approach in several contexts.[10]

MPC predicts future values of the process outputs based on a reasonably accurate dynamic model and provides the appropriate input signals by solving an optimization problem involving the computation of the optimum set points with constraints on inputs and outputs.[11] Garriga and Soroush,[12] presented a brief survey on various methods of control tuning in theoretical and practical aspects. Depending on applications and requirements, there exist different types of MPC algorithms like adaptive,[13] explicit,[14] robust,[15] economic,[16,17] stochastic,[18] distributed,[19] and so forth. Though MPC is advanced and embraces a predictive functionality, it lacks in the ease of industrial applications because of complex calculations within the sampling interval. This limitation laid the foundation toward the bridging of MPC and PID control schemes[20−23] through which MPC controller gain or closed-loop data is used to tune the PID parameters. As far as industrial implementation is concerned, the idea of bridging the advanced control mechanism and conventional controller spreads over in different aspects.[24] Preitl et al.[25] presented two iterative control schemes to formulate an objective function and validated with a PI controller. Vrkalovic et al.[26] had developed a model free sliding mode and PI-fuzzy controller using a Grey Wolf Optimizer.[27] In application toward optimization techniques, the teaching−learning-based optimization algorithm is applied to obtain the parameters of the fuzzy-PID controller.[28]

The method proposed here is a new PI controller tuning scheme using the closed-loop data of the extended predictive control (EPC) strategy. The controller parameters are obtained as a function of EPC manipulated variable response, time constant of the actual process, rise time of EPC unit step response, and condition number "r_2". In addition to the proposed control method, the mathematical modeling presented by Fedele[38] has been extended to multi input multi output (MIMO) processes. This paper is organized as follows: Section 2 presents a system description of the lab-scale distillation column and methodology of parameter estimation. The control design methodology is discussed in Section 3. Section 4 contains simulation results of parameter estimation using the procedure given in Section 2 and control scheme implementation on two case studies are presented with 30%

Received: August 22, 2019
Accepted: November 20, 2019
Published: December 5, 2019

© 2019 American Chemical Society

DOI: 10.1021/acsomega.9b02713
ACS Omega 2019, 4, 21230−21241

plant parameter uncertainty. The last section is devoted to conclusions.

2. SYSTEM DESCRIPTION AND MATHEMATICAL MODELING

The model is assumed as the first order plus dead time (FOPDT) structure throughout the paper, and the system is

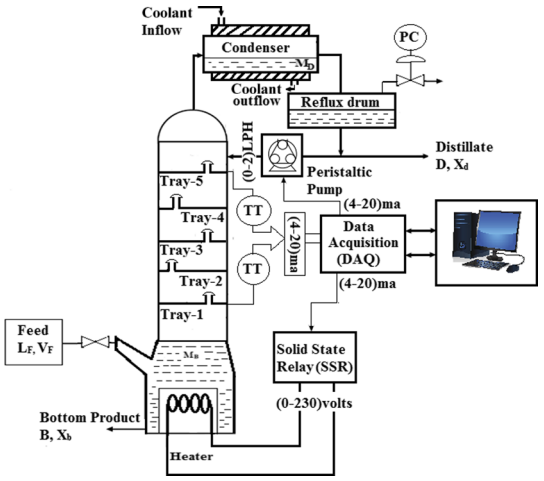

Figure 1. Schematic diagram of the distillation column.

assumed to be linear time-invariant at a certain operating region. The online binary distillation column is considered for this study with a feed mixture of 30% isopropyl alcohol and 70% water. The boiling point of isopropyl alcohol and water ranges as 81.5−82.5 °C[29] and 99−100 °C correspondingly. The intent is to separate this mixture and obtain maximum purity of isopropyl alcohol through the distillation process. Unlike the application in this paper, there are mixtures called azeotropes, which exhibits the same boiling point throughout the distillation process.[30] Alves et al.[31] presented a new approach for the prediction of azeotrope formation using neural networks. Figure 1 depicts the schematic diagram of the bubble cap distillation column. The column consists of five trays placed in the ascending order from bottom to top which are equidistant to each other. A heater with 4000 kW is fitted at the bottom of the column, which is manipulated using solid state relay, and there is an opening to inject the feed into the column. A condenser is located at the top of the column, which is used to cool down the hot vapor, which in turn converts it into the liquid state. There is a reflux drum at the outlet of the condenser which is used to collect condensed liquid, and a drum at the bottom end is used to collect the purified distillate. Reflux flow rate is manipulated by using a peristaltic pump (model: EnerTech ENPD 100). The sensors and final control elements are interfaced with the PC (configuration: HP ProDesk 400 G3 SFF, 4 GB RAM and 512 GB) using the data acquisition card. The mathematical modeling and controller execution have been realized through Matlab 2018a.

Temperature control is the crucial operation of distillation which influences the purity of the distillate.[32] If the temperature at a certain tray point in the system is too high or too low, expectable products or their quality may not be guaranteed.[33] Controlling of such systems is a challenge because of their nonlinear behavior. The control design is more complex because of its wide operating region of feed composition and flow rates. Model identification of such systems is difficult because of interaction in the process because of tray temperatures.[34,35] If the temperature at the top of the tower is more than what it should be, heavier components will be vaporized and become a part of the overhead product instead of flowing down as liquid and vice versa with lower temperatures.[36] Pressure is another parameter which influences the purity of distillate through the boiling temperature of liquid.

$$g_{ij}(s) = \frac{K_{ij}\, e^{-\theta_{ij} s}}{T_{ij}s + 1} \tag{1}$$

For the MIMO process, the overall system equation is

$$G = \begin{bmatrix} g_{11} & g_{12} & \cdot & \cdot & g_{1j} \\ g_{21} & \cdot & \cdot & \cdot & \cdot \\ \cdot & \cdot & \cdot & \cdot & g_{i-1j} \\ g_{i1} & \cdot & \cdot & g_{ij-1} & g_{ij} \end{bmatrix} \tag{2}$$

A linear regression approach is used to estimate system parameters through the equations that are obtained directly using the process output when the system is subjected to step change.[37] Unlike other least square methods which uses the process output from $t \geq \theta$, this approach considers process output from time where the step change U_0 is applied. The output of the process when step input is applied to eq 1 is given as

$$(Ts^2 + s)Y(s) = KU_0\, e^{-\theta s} \tag{3}$$

Differentiating eq 3 with respect to s results in

$$\frac{1}{\theta}\left[(2Ts + 1)Y(s) + (Ts^2 + s)\frac{dY(s)}{ds}\right] = -KU_0\, e^{-\theta s} \tag{4}$$

Summing up eqs 3 and 4

$$\theta(Ts^2 + s)Y(s) + (2Ts + 1)Y(s) + (Ts^2 + s)\frac{dY(s)}{ds} = 0 \tag{5}$$

To eliminate the derivatives of laplace "s", eq 5 is divided with s^2

$$T\left[2s^{-1}Y(s) + \frac{dY(s)}{ds}\right] + \theta s^{-1}Y(s) + \theta TY(s) = -s^{-2}Y(s) - s^{-1}\frac{dY(s)}{ds} \tag{6}$$

by applying inverse Laplace transform in eq 6

$$T\left[2\int_0^t y(\rho)d\rho - ty(t)\right] + \theta\int_0^t y(\rho)d\rho + \theta Ty(t) = -\int_0^t\int_0^\rho y(\lambda)d\lambda\, d\rho + \int_0^t \rho y(\rho)d\rho \tag{7}$$

Equation 7 can be rewritten as

$$Tg_1(t) + \theta g_2(t) + Lg_3(t) = g_4(t) \tag{8}$$

where, $\theta T = L$, $g_1(t) = 2\int_0^t y(\rho)d\rho - ty(t)$, $g_2(t) = \int_0^t y(\rho)d\rho$, $g_3(t) = y(t)$, $g_4(t) = -\int_0^t\int_0^\rho y(\lambda)d\lambda\, d\rho + \int_0^t \rho y(\rho)d\rho$.

The linear eq 8 allows the estimation of the unknown parameters "T" and "L" and the values of the auxiliary variable θ. To this aim, assume that $g_i(t)$, $i = 1, \ldots, 4$ are measured at times 0, $T_s, \ldots, (n-1)T_s$, where T_s is the sampling period and "n" is the number of samples, and it is defined as

DOI: 10.1021/acsomega.9b02713
ACS Omega 2019, 4, 21230−21241

$$x = [T \quad \theta \quad L]^{T} \tag{9}$$

$$\psi = \begin{bmatrix} g_1(0) & g_2(0) & g_3(0) \\ g_1(T_s) & g_2(T_s) & g_3(T_s) \\ . & . & . \\ . & . & . \\ g_1((n-1)T_s) & g_2((n-1)T_s) & g_3((n-1)T_s) \end{bmatrix} \tag{10}$$

and

$$\gamma = \begin{bmatrix} g_4(0) \\ g_4(T_s) \\ . \\ . \\ g_4((n-1)T_s) \end{bmatrix} \tag{11}$$

From eqs 9−11, eq 8 can be rewritten as

$$\psi x = \gamma \tag{12}$$

The estimation of parameters using least squares is obtained as

$$\hat{x} = (\psi^{T}\psi)^{-1}\psi^{T}\gamma \tag{13}$$

The system gain "K" is obtained by considering the steady state process output. Because there exist cases where the step stops before the steady state is reached, the parameter "K" has to be also identified during the plant transient response. To this aim, consider the step response of the process after $t = \theta$.

$$y(t) = KU_0(1 - e^{-(t-\theta)/T}), \quad t \geq \theta \tag{14}$$

Integrating $y(t)$ from $t = \theta$ to n

$$\int_{\theta}^{n} y(t)dt = U_0K(n - \theta - T + T\, e^{-(n-\theta)/T}) \tag{15}$$

From eq 15, process gain "K" can be obtained as

$$K = \frac{\int_{\theta}^{n} y(t)dt}{U_0(n - \theta - T + T\, e^{-(n-\theta)/T})} \quad n > \theta \tag{16}$$

The mathematical modeling approach has been implemented to estimate model parameters for the lab-scale distillation column as well as Wood and Berry plant.[39] Additional integral has been used in eq 7 to improve the filtering performance.

3. CONTROL DESIGN METHODOLOGY

A new control tuning method presented in this paper is carried out by considering the methodology of EPC and suppression matrix formulation.[40] In particular, PI controller gain parameters are computed by using closed-loop data of EPC.

Extending PID controller gains from the MPC approach is a contemporary method of the advanced control theory. There exists different aspects of formulating PID gains from MPC[20,41−44] Table 1 reports different PID formulations based on MPC.

The objective function to be minimized is defined over the prediction horizon (p), as a function of error and controller response for the servo operation. This objective function is minimized by evaluating a profile of manipulated input moves implemented at every sampling instant over the control horizon (m). The control law is based on the solution of the quadratic cost function using least squares with a weighting factor on the manipulated variable.

Table 1. Existing MPC-Based PID

authors	PID formulation
Yaun et al.[41]	$k_c = -(\widetilde{f_1} + 2\widetilde{f_2})$
	$T_i = -\frac{\widetilde{f_1} + 2\widetilde{f_2}}{\widetilde{f_0} + \widetilde{f_1} + \widetilde{f_2}} T_s$
	$T_d = -\frac{\widetilde{f_2}}{(\widetilde{f_1} + 2\widetilde{f_2})} T_s$
Abdelrauf et al.[43]	$k_p = e(k) - e(k-1)$
	$k_i = t_s e(k)$
	$k_d = \frac{1}{t_s}[e(k) - 2e(k-1) + e(k-2)]$
Johnson and Moradi[42]	$k_p = -2K_1(k) - K_2$
	$k_i = K_1(k) + K_2(k) + K_3(k)$
	$k_d = K_1$
Sato et al.[44]	$k_c[k] = -f_1 - 2f_2 - g_1k_c[k-1] - \ldots - g_mk_c[k-m]$
	$T_i = \frac{f_1 + 2f_2}{f_0 - p_y + f_1 + f_2} T_s$
	$T_d = -\frac{f_2}{f_1 + 2f_2} T_s$
Tan et al.[20]	$k_p = -(K_1(k) + K_2(k))$
	$k_i = -K_3(k)$
	$k_d = K_1(k)$

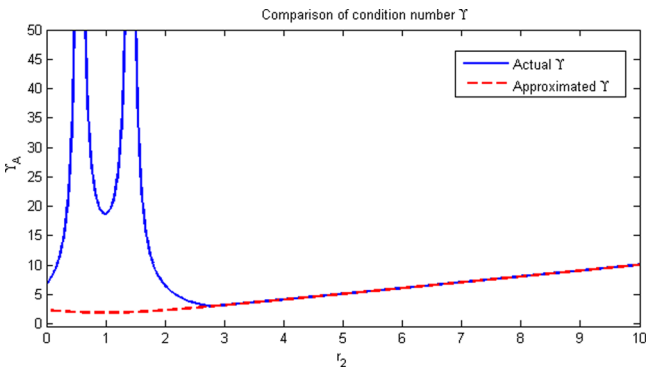

Figure 2. Condition number comparison of actual and approximated.

$$\min_{\Delta u} J = [e - A\Delta u]^{T}[e - A\Delta u] + \Delta u^{T}\lambda\Delta u \tag{17}$$

In this paper, an infinite horizon control problem is considered to formulate the predictive algorithm. The unconstrained MPC control law is given by[45]

$$\Delta u = (A^{T}A + \lambda I)^{-1}A^{T}e \tag{18}$$

where "A" is a dynamic matrix obtained from the step response coefficients of individual transfer function (g_{ij}), where "i" is the output and "j" is the input of the process. "λ" is a suppression weighting factor, "e" is the vector of tracking difference between trajectory reference and the prediction of the process. "λI" of eq 18 is considered as the extended moving suppression matrix and it is represented as W_{EMS}. For "n" step prediction (n = runtime), system matrix "A" of the MIMO process for "N" inputs and "M" outputs is given by

DOI: 10.1021/acsomega.9b02713
ACS Omega 2019, 4, 21230−21241

$$A = \begin{bmatrix} a_{1,1}^{1} & 0 & \dots & 0 & a_{1,1}^{M} & 0 & \dots & 0 \\ a_{1,2}^{1} & a_{1,1}^{1} & \dots & 0 & a_{1,2}^{M} & a_{1,1}^{M} & \dots & 0 \\ \vdots & \vdots & \vdots & \vdots & \vdots & \vdots & \vdots & \vdots \\ a_{1,p}^{1} & a_{1,p-1}^{1} & \dots & a_{1,p-m+1}^{1} & a_{1,p}^{M} & a_{1,p-1}^{M} & \dots & a_{1,p-m+1}^{M} \\ & & & & \ddots & & & \\ a_{N,1}^{1} & 0 & \dots & 0 & a_{N,1}^{M} & 0 & \dots & 0 \\ a_{N,2}^{1} & a_{N,1}^{1} & \dots & 0 & a_{N,2}^{M} & a_{N,1}^{M} & \dots & 0 \\ \vdots & \vdots & \vdots & \vdots & \vdots & \vdots & \vdots & \vdots \\ a_{N,p}^{1} & a_{N,p-1}^{1} & \dots & a_{N,p-m+1}^{1} & a_{N,p}^{M} & a_{1,p-1}^{M} & \dots & a_{1,p-m+1}^{M} \end{bmatrix} \quad (19)$$

For the two input two output (TITO) process, eq 19 can be rewritten as

$$A = \begin{bmatrix} A_{11} & A_{12} \\ A_{21} & A_{22} \end{bmatrix} \quad (20)$$

The weighting matrix W_{EMS} is formulated by considering the same even elements of the first row to improve the ill conditioning of the weighting matrix. For the TITO process, W_{EMS} is given as

$$W_{EMS}^{MIMO} = \begin{bmatrix} W_1 & 0 \\ 0 & W_2 \end{bmatrix} \quad (21)$$

From eq 21

$$W_1 = \begin{bmatrix} 0 & -\beta_1 & \frac{-\beta_1}{R_1} \\ -\beta_1 & 0 & -r_1\beta_1 \\ \frac{-\beta_1}{R_1} & -r_1\beta_1 & 0 \end{bmatrix} \quad W_2 = \begin{bmatrix} 0 & -\beta_2 & \frac{-\beta_2}{R_1} \\ -\beta_2 & 0 & -r_1\beta_2 \\ \frac{-\beta_2}{R_1} & -r_1\beta_2 & 0 \end{bmatrix}$$

for $m = 3$.

The tuning parameters r_1 and r_2 are tuned independently based on the corresponding step response coefficient matrices A_{11} and A_{22}. Initially, r_2 is tuned using condition number γ through independent matrix A_{22}. The condition number of $(A^TA + W_{EMS})^{-1}$ is obtained as

$$\gamma = \|A^TA + W_{EMS}\| \, \|(A^TA + W_{EMS})^{-1}\| \quad (22)$$

and approximated condition number γ_{approx} using weighting ratio "r" and weighting factor R_1 is given as

$$\gamma_{approx} = 1 + \sqrt{r^2 - 2r + 2 - \left(\frac{2}{R_1} - \frac{1}{R_1^2}\right)} \quad (23)$$

The analysis to formulate eqs 22 and 23 is presented by Abu-Ayyad et al.[46] through a relatively lower condition number that depicts a smaller move suppression value.

The value where condition number γ and approximated condition number γ_{approx} overlaps is considered as the tuning value of r_2. Later, using r_2, the tuning parameter r_1 is chosen. The actual and approximated condition number comparison is shown in Figure 2. The tuning parameter R_1 is considered as "10" for all processes. Another tuning parameter "β" is obtained using the initial element of matrix "A^TA" from individual submatrices (A_{11} and A_{22}).

3.1. Formulation of PI Formula from EPC Control. The EPC algorithm is performed using eq 18 for unit step input in offline considering the process as an infinite prediction horizon problem ($p = n$). Proportional gain is computed by summing up the magnitude change of controller output "Δu" for all time samples of EPC response till its settling time. Integral gain is obtained as a function of proportional gain and rise time "T_r" of EPC unit step response.

Proportional gain

$$K_{Pi} = \frac{\delta_i \sum_{k=1}^{T_s} \Delta u_i(k)}{r_2} \quad i = 1,2, \dots, z \quad (24)$$

where "i" denotes the loop number (zth loop), δ is a tuning parameter selected as the maximum value of the off-diagonal time constant for loop-1 and the minimum value of the diagonal time constant for loop-2, that is,

$$\delta_1 = \max T(G_{12}, G_{21})$$

$$\delta_2 = \min T(G_{11}, G_{22})$$

"T_s" is the settling time of EPC closed-loop response and "Δu" is the change in controller output. r_2 is the intersection value of the actual and approximated condition number (γ).

Integral gain

$$K_{Ii} = \frac{K_{Pi}}{T_{ri}\alpha_i} \quad i = 1,2, \dots, z \quad (25)$$

where "T_r" is rise time and "α" is the tuning parameter that employs the speed of the process ranging (0,1). The pace of the process is directly proportional to offline EPC response for unit step input. Tuning parameter "δ" for the single input single output (SISO) process is selected as the time constant "T" of the FOPDT model.

4. RESULTS AND DISCUSSION

In this section, parameter estimation and validation of the control tuning method has been carried out by considering two case studies of MIMO processes. The proposed method has been compared with GPC−PID and hybrid control methods. Performance indices using integral time absolute error (ITAE) is presented with 30% uncertainty on all plant model parameters.

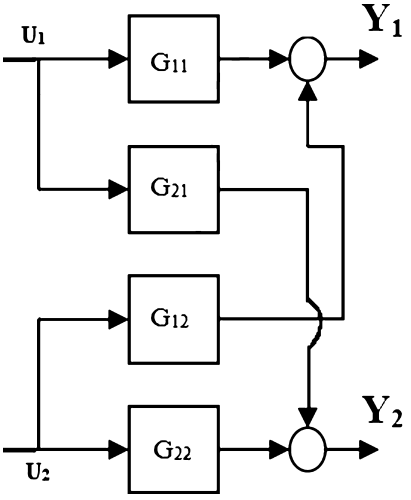

Figure 3. Open loop block diagram representation for the TITO process.

DOI: 10.1021/acsomega.9b02713
ACS Omega 2019, 4, 21230−21241

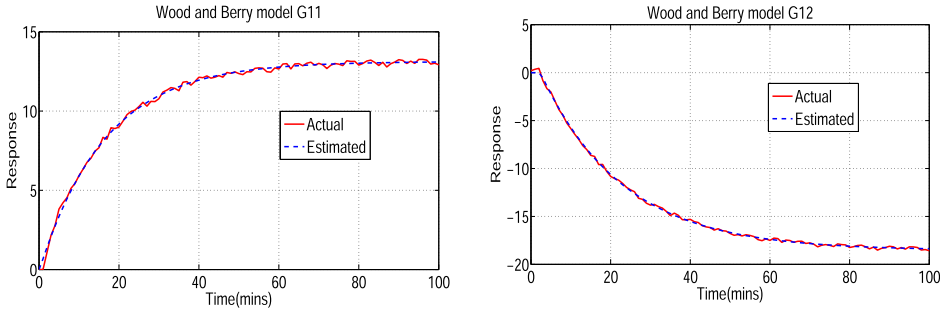

(a) Open loop response of G_{11} (b) Open loop response of G_{12}

Figure 4. G_{11} and G_{12} open loop response of the WB model.

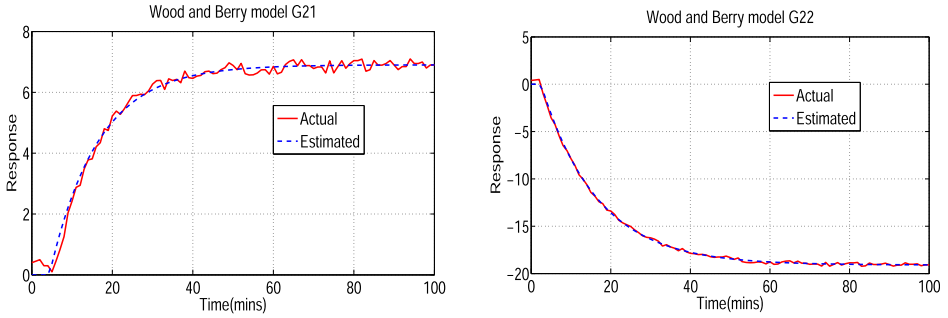

(a) Open loop response of G_{21} (b) Open loop response of G_{22}

Figure 5. G_{21} and G_{22} open loop response of the WB model.

Table 2. Comparison of Estimated Model Parameters for the WB Model with the Actual Model

parameters	actual model parameters	estimated model parameters	absolute error	error (%)
K_{11}	12.8	12.78	0.02	0.15
T_{11}	16.7	16.65	0.05	0.29
θ_{11}	1	1.04	0.04	4
K_{12}	−18.9	−18.92	0.02	0.1
T_{12}	21	21.04	0.04	0.19
θ_{12}	3	2.97	0.03	1
K_{21}	6.6	6.575	0.025	0.37
T_{21}	10.9	10.75	0.15	1.37
θ_{21}	7	7.18	0.18	2.57
K_{22}	−19.4	−19.42	0.02	0.1
T_{22}	14.4	14.45	0.05	0.34
θ_{22}	3	2.97	0.03	1

4.1. Parameter Estimation. The estimation of model parameters has been carried out on two case studies (case-1: Wood and Berry model[39] and case-2 experimental distillation setup[17]). The methodology presented in Section 2 is used to estimate the model parameters.

4.1.1. Parameter Estimation Case-1: Wood and Berry Model Estimation. The Wood and Berry model is considered as the benchmark for illustrating the MIMO process. The model estimation is carried out by considering the composition of the overhead and bottom product as process variables with reflux flow and steam flow as manipulated inputs. It has been proven to be a difficult process to control because of an interaction effect between the input−output variables. The true model has been depicted in eq 26.

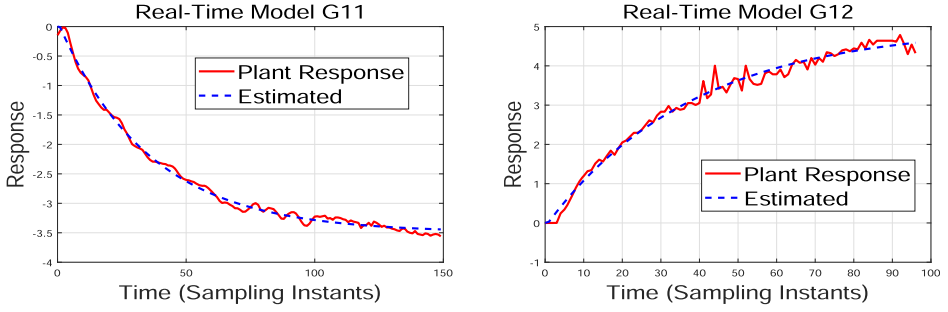

(a) Open loop response of G_{11} (b) Open loop response of G_{12}

Figure 6. G_{11} and G_{12} open loop response of the experimental system.

DOI: 10.1021/acsomega.9b02713
ACS Omega 2019, 4, 21230−21241

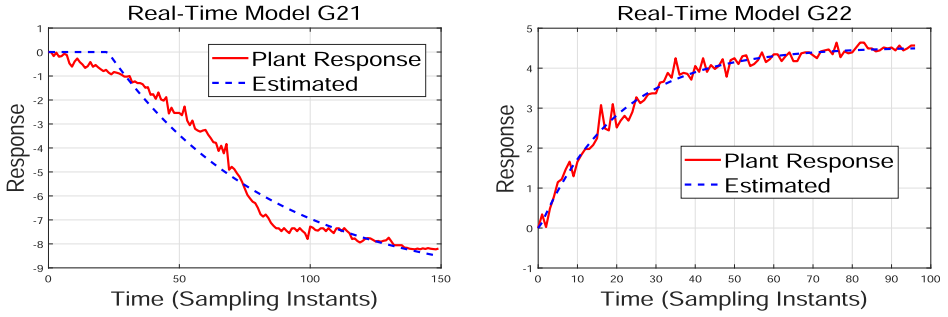

(a) Open loop response of G21 (b) Open loop response of G_{22}

Figure 7. G_{21} and G_{22} open loop response of the experimental system.

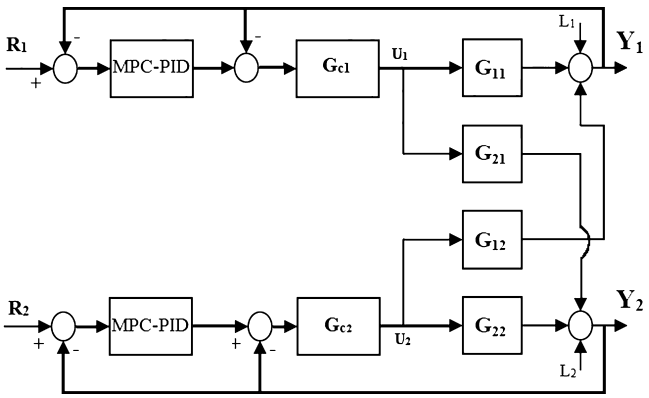

Figure 8. Decentralized control structure with a decoupler, where, $D_{11} = D_{22} = 1$, $D_{21} = -G_{21}/G_{22}$, and $D_{12} = -G_{12}/G_{11}$.

$$G(s) = \begin{bmatrix} \frac{12.8e^{-1s}}{16.7s+1} & \frac{-18.6e^{-3s}}{21s+1} \\ \frac{6.6e^{-7s}}{10.9s+1} & \frac{-19.4e^{-3s}}{14.4s+1} \end{bmatrix} \quad (26)$$

The step response data for the Wood and Berry (WB) plant is obtained by performing two experiments with unit step input sequentially for both the inputs (U_1 and U_2). Figure 3 depicts the block diagram of the open loop TITO process.

Step response data of eq 26 are used to estimate the model parameters subjected to eqs 8 and 16. Figures 4 and 5 depict fit test responses of the estimated model.

It is to be noted that to replicate simulation response of the WB model as actual measurement response, the plant outputs are corrupted with random Gaussian noise with zero mean and variance as a factor of 0.05 magnitude. Table 2 depicts the comparison of model parameters with absolute error and error percentage.

Therefore the estimated model is given as

$$\hat{G}(s) = \begin{bmatrix} \frac{12.78e^{-1.04s}}{16.65s+1} & \frac{-18.92e^{-2.97s}}{21.04s+1} \\ \frac{6.575e^{-7.18s}}{10.75s+1} & \frac{-19.42e^{-2.97s}}{14.45s+1} \end{bmatrix} \quad (27)$$

4.1.2. Parameter Estimation Case-2: Lab-Scale Distillation Column. A highly interactive lab-scale distillation column (Figure 17) is considered for the experimental study to estimate the model parameters. The two tray temperatures (tray-1 and tray-5) are considered as process variables with heater voltage (Q_h) and reflux flow rate (L_r) as manipulated inputs correspondingly. The step test has been performed for both the inputs sequentially by manipulating one input change at a time. Figures 6 and 7 show fit test of the lab-scale distillation column.

The initial manipulated input are considered as, $[L_r, Q_h] = [10, 50]\%$. For step-1, the inputs are excited from $[10, 50]$ to $[35, 50]\%$ and corresponding response at Y_1 and Y_2 is observed. Similarly, for step-2, the inputs are excited from $[10, 50]$ to $[10, 75]\%$.

Note that because of steady state requirement, the step response time with step change in reflux flow rate is more than the step change-applied heater voltage with respect to the variable of interest.

The model estimated by using eqs 8 and 16 is

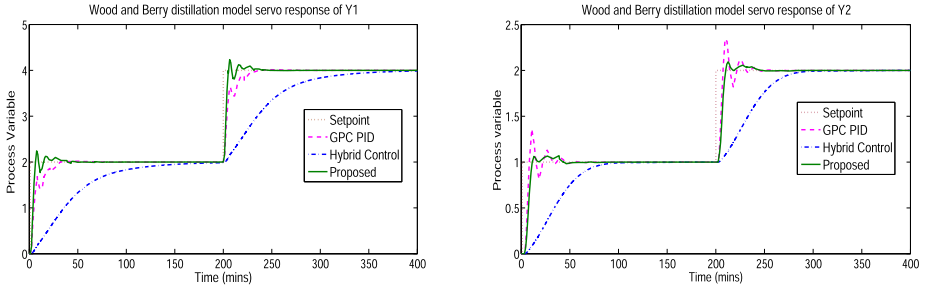

(a) Servo response comparison of Y_1 for WB model (b) Servo response comparison of Y_2 for WB model

Figure 9. Process variable simulation response comparison of Y_1 and Y_1 for the WB model.

DOI: 10.1021/acsomega.9b02713
ACS Omega 2019, 4, 21230−21241

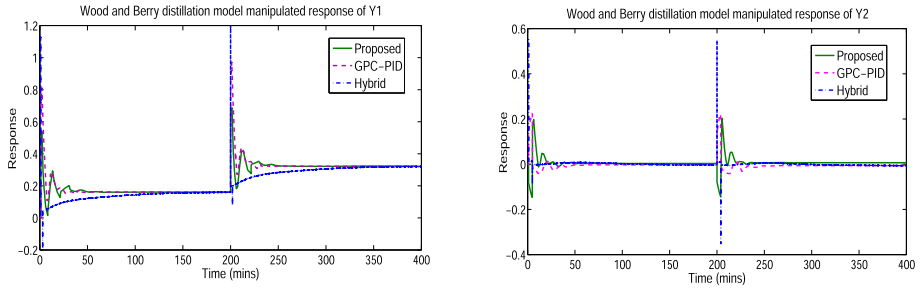

(a) Manipulated variable responses comparison of Y_1 for WB model

(b) Manipulated variable responses comparison of Y_2 for WB model

Figure 10. Manipulated variable response comparison of Y_1 and Y_2 for the WB model.

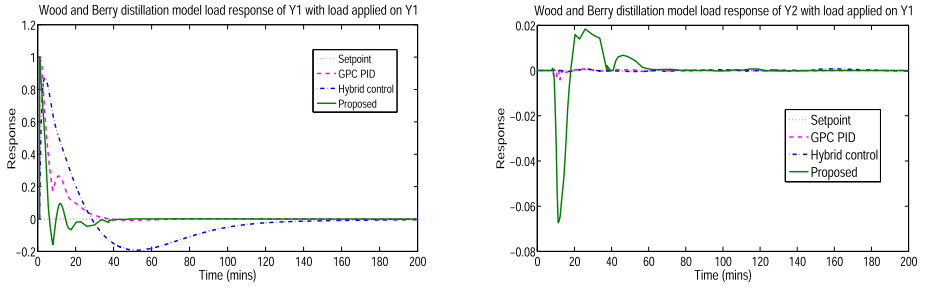

(a) Regulatory response of Y_1 when load is applied on Y_1

(b) Regulatory response of Y_2 when load is applied on Y_1

Figure 11. Regulatory response of Y_1 and Y_2 when load (d_1) is applied on Y_1.

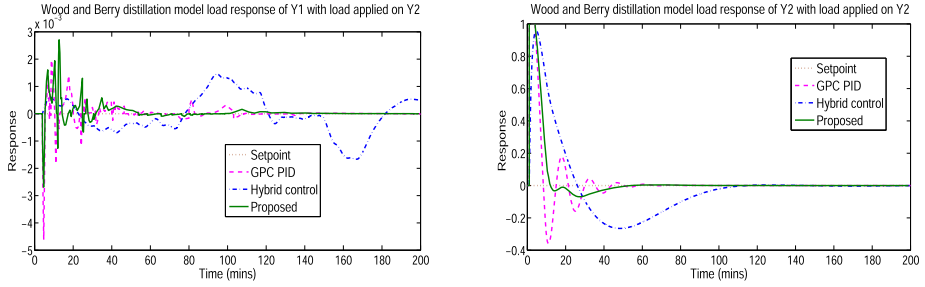

(a) Regulatory response of Y_1 when load is applied on Y_2

(b) Regulatory response of Y_2 when load is applied on Y_2

Figure 12. Regulatory response of Y_1 and Y_2 when load is applied on Y_2.

Table 3. ITAE Values of the WB Model with Uncertainty (Servo Operation)

	methods	main	interaction	total
C-1	GPC−PID	126.48	11.32	137.8
	hybrid	7089	1.98	7090.98
	proposed	105.26	5.91	111.17
C-2	GPC−PID	416.52	201.7	618.22
	hybrid	3252.4	460.4	3712.8
	proposed	191.4	159.82	350.96
C-3	GPC−PID	380.3	163.29	543.59
	hybrid	3229.1	628.9	3858
	proposed	322.12	267.56	589.68
C-4	GPC−PID	388.25	197.19	585.44
	hybrid	3206.2	614.2	3820.4
	proposed	291.56	258.02	549.58

Table 4. ITAE Values of the WB Model with Uncertainty (Load Operation)

	methods	main	interaction	total
C-1	GPC−PID	126.82	12.02	138.84
	hybrid	942.3	2.29	944.59
	proposed	105.36	5.77	111.13
C-2	GPC−PID	420.4	210.7	631.1
	hybrid	1600	1241	2841
	proposed	191.02	159.77	350.79
C-3	GPC−PID	380.4	162.99	543.39
	hybrid	2221.1	2132.906	4354.006
	proposed	321.9	267.37	589.27
C-4	GPC−PID	386.24	201.69	587.93
	hybrid	2153.2	1697.8	3851
	proposed	291.37	255.74	547.11

DOI: 10.1021/acsomega.9b02713
ACS Omega 2019, 4, 21230−21241

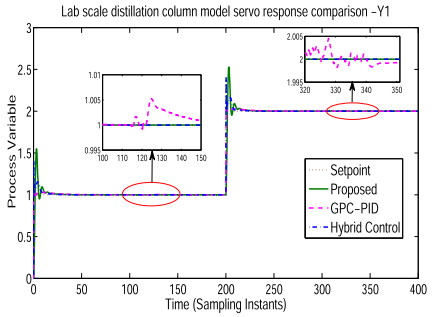

(a) Servo response comparison of Y_1 for lab scale distillation column model

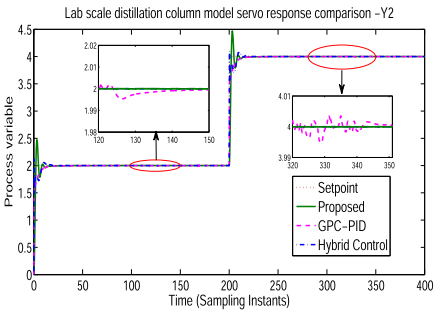

(b) Servo response comparison of Y_2 for lab scale distillation column model

Figure 13. Process variable responses of Y_1 and Y_2 for the lab-scale distillation column.

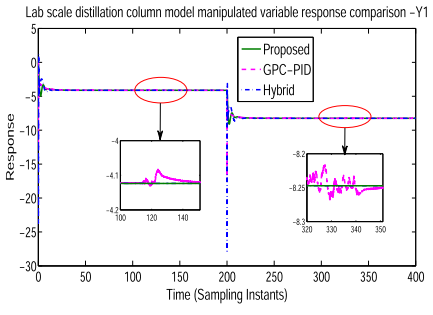

(a) Manipulated variable responses comparison of Y_1 for lab scale distillation column model

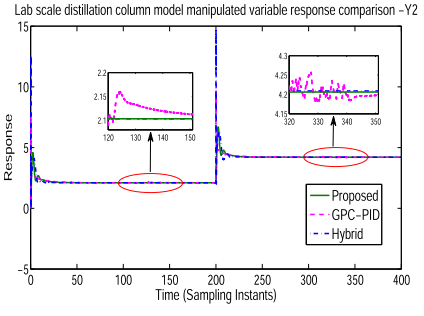

(b) Manipulated variable responses comparison of Y_2 for lab scale distillation column model

Figure 14. Manipulated variable responses of Y_1 and Y_2 for the lab-scale distillation column.

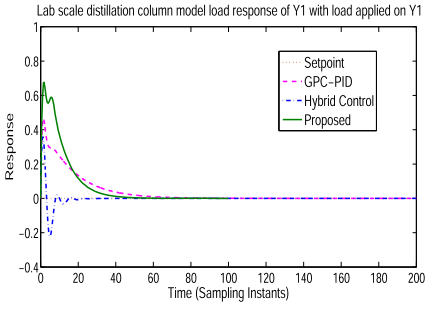

(a) Regulatory response of Y_1 when load is applied on Y_1

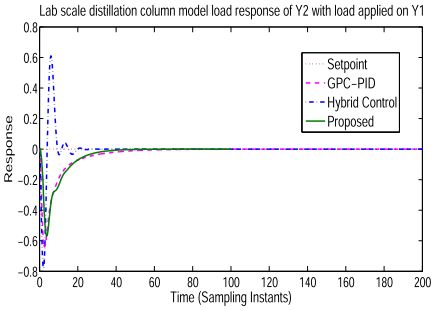

(b) Regulatory response of Y_2 when load is applied on Y_1

Figure 15. Regulatory response of Y_1 and Y_2 when load is applied on Y_1 (pilot plant model).

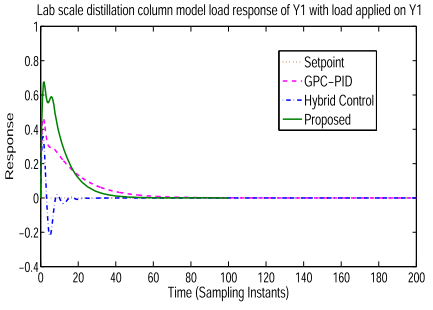

(a) Regulatory response of Y_1 when load is applied on Y_2

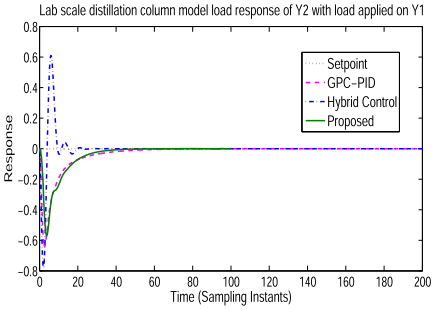

(b) Regulatory response of Y_2 when load is applied on Y_2

Figure 16. Regulatory response of Y_1 and Y_2 when load is applied on Y_2 (pilot plant model).

DOI: 10.1021/acsomega.9b02713
ACS Omega 2019, 4, 21230−21241

Table 5. ITAE Values of the Pilot Plant Model with Uncertainty (Servo Operation)

	methods	main	interaction	total
C-1	GPC−PID	146.45	125.17	271.62
	hybrid	60.28	59.78	120.06
	proposed	60.78	53.64	114.42
C-2	GPC−PID	156.07	143.07	299.14
	hybrid	66.47	65.86	132.33
	proposed	63.99	61.33	125.32
C-3	GPC−PID	152.02	139.4	291.42
	hybrid	77.04	82.41	159.45
	proposed	60.02	57.75	117.77
C-4	GPC−PID	152.6	139.96	292.56
	hybrid	64.15	68.98	133.53
	proposed	60.55	58.21	118.76

Table 6. ITAE Values of the Pilot Plant Model with Uncertainty (Load Operation)

	methods	main	interaction	total
C-1	GPC−PID	157.42	134.94	291.91
	hybrid	40	40	80
	proposed	70.61	61.42	132.03
C-2	GPC−PID	168.49	154.32	322.91
	hybrid	50.82	50.66	101.48
	proposed	74.14	69.85	143.99
C-3	GPC−PID	163.72	149.83	313.57
	hybrid	79.6	81.55	161.15
	proposed	70.19	66.32	136.51
C-4	GPC−PID	164.39	150.42	314.81
	hybrid	70.65	73.83	144.48
	proposed	70.64	66.7	137.34

$$\hat{G}(s) = \begin{bmatrix} Y_1(\text{tray 5}) \\ Y_2(\text{tray 1}) \end{bmatrix} = \begin{bmatrix} \frac{-0.1406e^{-0.0142s}}{0.5985s+1} & \frac{0.1998e^{-0.012s}}{0.6333s+1} \\ \frac{-0.3929e^{-0.16s}}{1.04s+1} & \frac{0.1806e^{-0.006s}}{0.3191s+1} \end{bmatrix} \begin{bmatrix} L_r \\ Q_h \end{bmatrix} \quad (28)$$

4.2. Implementation of Control Schemes. The decentralized control structure with a decoupler shown in Figure 8 is considered for the simulation and comparison of the proposed controller with GPC−PID,[42,47] and the hybrid control approach[41] has been used. Simulation is executed with servo and regulatory operations under 30% plant parameter uncertainties in "K", "τ", and "θ".

4.2.1. Case Study-1: Wood and Berry Model. 4.2.1.1. Servo Operation. The Wood and Berry model is subjected to closed-loop simulation with set point step changes of [2,4], applied at time (0,200) min for loop-1. The response is observed at Y_1, as shown in Figure 9a, and for loop-2, the response of process variable Y_2 with set point step changes of [1,2], applied at time (0,200) min, is represented in Figure 9b. Correspondingly, manipulated variable responses of loop-1 and loop-2 are shown in Figure 10a,b, respectively. The controller parameters using GPC-PID and proposed methodology for Wood and Berry model is given in Table 7 and Table 8, respectively.

4.2.1.2. Regulatory Operation. Load on both the loops are imposed individually at the zero steady state, as shown in Figure 8. When load (L_1) is applied at output Y_1, the effect observed on output Y_1 is quoted as the main effect, and the effect observed on output Y_2 is the interaction effect to the load at Y_1. It is the same in the case of load (L_2) on Y_2 as well. Figure 11a depicts the response of Y_1 when load is applied at Y_1. For the same load at Y_1, the response of Y_2 is shown in Figure 11b.

Similarly, Figure 12a depicts the response of Y_1 when load is applied at Y_2. For the same load at Y_2, the response of Y_2 is shown in Figure 12b.

4.2.1.3. Performance Indices. When determining the performance of the controller, it is often helpful to consider how "large" the error from the setpoint is. ITAE is one of the criteria that are used to evaluate the controller performance by essentially adding errors at every sampling instant over a period of run-time. System perturbation is one aspect of determining the efficiency of the controller. In this paper, plant parameters are perturbed with 30% uncertainty in all individual model parameters with four cases (C-1 is nominal plant; C-2 is 30% uncertainty in "K"; C-3 is 30% uncertainty in "K" and "T"; and C-4 is 30% uncertainty in "K", "T", and θ). Table 3 refers to servo operation performance of the Wood and Berry model with plant uncertainties for different control schemes.

Table 4 depicts the ITAE values of the WB model subjected to regulatory operation in comparison with different control schemes under plant uncertainties.

4.2.2. Case Study-2: Lab-Scale Distillation Column Model. 4.2.2.1. Servo Operation. Lab-scale plant model 27 is subjected to closed-loop simulation with set point step changes of (1,2) applied at time (0,200) min for loop-1. The response is observed at Y_1 as shown in Figure 13a. Similarly, for loop-2, set point step changes of (2,4) is applied at time (0,200) min and the response is observed at Y_2 depicted in Figure 13b. Manipulated variable response of loop-1 and loop-2 is given in Figure 14a,b respectively. The controller parameters using GPC-PID and proposed methodology for pilot-Scale Distillation Column Model is given in Table 9 and Table 10, respectively.

4.2.2.2. Regulatory Operation. The load on both the loops is imposed individually on the initial state of system at zeroth sampling instant. Figure 15a depicts the response of Y_1 when load is applied at Y_1. For the same load at Y_1, the response of Y_2 is shown in Figure 15b.

Similarly, Figure 16a depicts the response of Y_1 when load is applied at Y_2. For the same load at Y_2, the response of Y_2 is shown in Figure 16b.

4.2.2.3. Performance Indices. Table 5 refers to ITAE values of servo operation of the pilot-scale plant model with plant uncertainties in comparison with different control schemes. Table 6 depicts the ITAE values of the pilot-scale plant model subjected to regulatory operation in comparison with different control schemes under plant uncertainties.

Overall performance of hybrid control is efficient compared to the proposed algorithm in case of nominal and uncertainty in "K" but lags when uncertainty is introduced in "T" and θ cases. Through the performance index, it has been observed that the proposed control scheme is effective compared to GPC−PID and hybrid control schemes.

5. CONCLUSIONS

In this work, the parameter estimation using the regression method has been carried out, and the obtained model is in the form of the FOPDT structure. The development of a new PI control tuning approach has been presented from the EPC strategy. The controller parameters are formulated from

DOI: 10.1021/acsomega.9b02713
ACS Omega 2019, 4, 21230−21241

summation of instantaneous controller changes and rise time of the closed-loop unit step response of EPC. The application of this novel design has been demonstrated through benchmark and experimental models of the distillation process. Performance analysis has been carried out to depict the efficiency of the controller under plant uncertainty and compared with other well-accepted control schemes.

6. EXPERIMENTAL IMPLEMENTATION AND ANALYSIS

The proposed controller has been implemented on the experimental setup shown in Figure 17 to control coupled tray temperature.

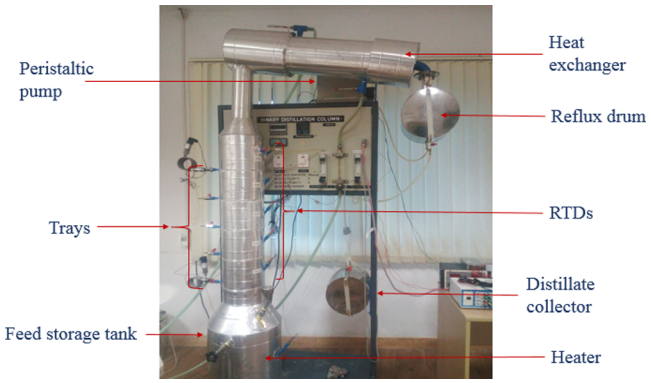

Figure 17. Lab-scale binary distillation column (available in lab-2, ICE dept, MIT, Manipal).

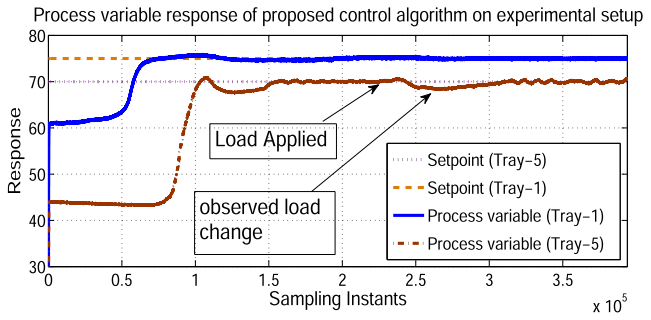

Figure 18. Experimental response of process variables for the proposed controller.

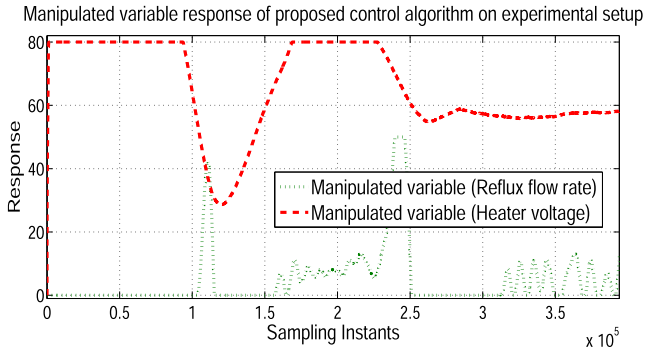

Figure 19. Experimental response of manipulated variables for the proposed controller.

Figures 18 and 19 depict process variables and manipulated variable response of the lab-scale distillation column. The operating region of tray temperature was initialized at [61, 44] °C and the proposed controller was implemented with set points of [75, 70] °C for tray-1 and tray-5, respectively. As the system reached the desired state, the pressure valve on the reflux drum is disturbed to observe the regulatory operation. In rejecting the load disturbance, the controller effect has been observed on both the manipulated inputs.

There is an arrangement of the pressure knob on the reflux drum which is used to release excess pressure in the column. The system is perturbed with an external disturbance by releasing pressure manually using the pressure knob, and the regulatory response effecting temperature of tray-5 is observed. When the disturbance is applied at 2.25×10^4 sampling instant, the effect of the load is observed at 2.65×10^4 sampling instant (because temperature control is a slow process). While controlling tray temperature, the controller tends toward saturation because of integral windup. To overcome integral windup, a conditional integrator approach[3] is used within the control loop.

APPENDIX

Wood and Berry decoupler model

$$D_{WB} = \begin{bmatrix} 1 & \dfrac{(315.63s + 18.9)e^{-2\cdot s}}{268.8s + 12.8} \\ \dfrac{(95.04s + 6.6)e^{-4\cdot s}}{211.46s + 12.8} & 1 \end{bmatrix}$$

Pilot-scale distillation column decoupler model

$$D_{PSDC} = \begin{bmatrix} 1 & \dfrac{0.1195s + 0.1998}{0.088s + 0.1406} \\ \dfrac{(0.1253s + 0.3929)e^{-0.16\cdot s}}{0.1892s + 0.1806} & 1 \end{bmatrix}$$

Controller Gain Parameters

Wood and Berry decoupler model (Tables 7 and 8):

Table 7. GPC−PID Controller: Wood and Berry

parameters	loop-1	loop-2
K_P	0.3886	−0.168
K_I	0.0932	−0.012
K_D	0.527	−0.161

Table 8. Proposed Controller: Wood and Berry

parameters	loop-1	loop-2
K_P	0.347	−0.091
K_I	0.0662	−0.0212

Pilot-scale distillation column model (Tables 9 and 10):

AUTHOR INFORMATION

Corresponding Author

*E-mail: itarasu@manipal.edu. Phone: +91 974 073 1983.

Table 9. GPC−PID Controller: Pilot-Scale Distillation Column

parameters	loop-1	loop-2
K_P	−8.02	3.67
K_I	−0.937	1.198
K_D	−2.574	3.943

DOI: 10.1021/acsomega.9b02713
ACS Omega 2019, 4, 21230−21241

Table 10. Proposed Controller: Pilot-Scale Distillation Column

parameters	loop-1	loop-2
K_p	−1.1056	0.6879
K_I	−0.9641	1.7533

ORCID

Eadala Sarath Yadav: 0000-0001-7157-5395

Notes

The authors declare no competing financial interest.

■ ACKNOWLEDGMENTS

The first author would like to acknowledge the Manipal Academy of Higher Education for providing stipend under TMA Pai scholarship toward this experimental research work. The authors would like to thank the department of Instrumentation and Control Engineering, Manipal Institute of Technology, for providing the experimental facility. Our special thanks to Dr. J. Prakash, Anna University, Tamilnadu, India, for timely suggestions and guidance in this work. We would also like to thank Dr. R. Russell Rhinehart, Professor Emeritus, Chemical Engineering, Oklahoma State University, Stillwater, USA, for the technical inputs to improve the paper.

■ NOMENCLATURE

θ	dead time
C-1	nominal plant
C-2	uncertainty in "K"
C-3	uncertainty in "K" and "T"
C-4	uncertainty in "K", "T", and "θ"
EPC	extended predictive control
GPC	generalized predictive control
IO	input−output
ITAE	integral time absolute error
K	process gain
L_r	reflux flow rate
m	control horizon
MIMO	multi input multi output
MPC	model predictive control
n	total run-time
p	prediction horizon
PID	proportional integral and derivative
PSDC	pilot-scale distillation column
Q_h	heater voltage
SISO	single input single output
T	time constant
T_s	sampling interval
TITO	two input two output
TT	temperature transmitter
WB	Wood and Berry
X_b	bottom product concentration (mol/h)
X_d	distillate concentration (mol/h)

■ REFERENCES

(1) Åström, K. J.; Hägglund, T.*Advanced PID Control*; ISA-The Instrumentation, Systems, and Automation Society Research Triangle, 2006; pp 1−10.

(2) Majhi, S.; Atherton, D. P. Modified Smith predictor and controller for processes with time delay. *IEE Proc. Control Theory Appl.* **1999**, *146*, 359−366.

(3) Visioli, A. *Practical PID Control*; Springer Science & Business Media, 2006; pp 1−18.

(4) García, C. E.; Prett, D. M.; Morari, M. Model predictive control: theory and practiceâĂŤa survey. *Automatica* **1989**, *25*, 335−348.

(5) Sung, S. W.; Lee, I.-B. Limitations and countermeasures of PID controllers. *Ind. Eng. Chem. Res.* **1996**, *35*, 2596−2610.

(6) Bielecki, T. R.; Chen, T.; Cialenco, I.; Cousin, A.; Jeanblanc, M. Adaptive robust control under model uncertainty. *SIAM J. Control Optim.* **2019**, *57*, 925−946.

(7) Liu, G. P.; Daley, S. Optimal-tuning PID control for industrial systems. *Contr. Eng. Pract.* **2001**, *9*, 1185−1194.

(8) Ioannou, P. A.; Sun, J. *Robust Adaptive Control*; Courier Corporation, 2012; pp 5−23.

(9) Zhu, Y.; Zhao, D.; He, H.; Ji, J. Event-triggered optimal control for partially unknown constrained-input systems via adaptive dynamic programming. *IEEE Trans. Ind. Electron.* **2016**, *64*, 4101−4109.

(10) Rawlings, J. B.; Mayne, D. Q. *Model Predictive Control: Theory and Design*; Nob Hill Pub: Madison, Wisconsin, 2009; pp 1−60.

(11) Qin, S. J.; Badgwell, T. A. A survey of industrial model predictive control technology. *Contr. Eng. Pract.* **2003**, *11*, 733−764.

(12) Garriga, J. L.; Soroush, M. Model predictive control tuning methods: A review. *Ind. Eng. Chem. Res.* **2010**, *49*, 3505−3515.

(13) Adetola, V.; DeHaan, D.; Guay, M. Adaptive model predictive control for constrained nonlinear systems. *Syst. Control Lett.* **2009**, *58*, 320−326.

(14) Tøndel, P.; Johansen, T. A.; Bemporad, A. An algorithm for multi-parametric quadratic programming and explicit MPC solutions. *Automatica* **2003**, *39*, 489−497.

(15) Pluymers, B.; Rossiter, J. A.; Suykens, J. A. K.; De Moor, B. A simple algorithm for robust MPC. *IFAC Proc. Vol.* **2005**, *38*, 257−262.

(16) Touretzky, C. R.; Baldea, M. Integrating scheduling and control for economic MPC of buildings with energy storage. *J. Process Control* **2014**, *24*, 1292−1300.

(17) Hovgaard, T. G.; Edlund, K.; Jørgensen, J. B. The potential of economic MPC for power management. *49th IEEE Conference on Decision and Control (CDC)*, 2010; pp 7533−7538.

(18) Di Cairano, S.; Bernardini, D.; Bemporad, A.; Kolmanovsky, I. V. Stochastic MPC with learning for driver-predictive vehicle control and its application to HEV energy management. *IEEE Trans. Control Syst. Technol.* **2013**, *22*, 1018−1031.

(19) Alvarado, I.; Limon, D.; Muñoz de la Peña, D.; Maestre, J. M.; Ridao, M. A.; Scheu, H.; Marquardt, W.; Negenborn, R. R.; De Schutter, B.; Valencia, F.; et al. A comparative analysis of distributed MPC techniques applied to the HD-MPC four-tank benchmark. *J. Process Control* **2011**, *21*, 800−815.

(20) Tan, K. K.; Lee, T. H.; Huang, S. N.; Leu, F. M. PID control design based on a GPC approach. *Ind. Eng. Chem. Res.* **2002**, *41*, 2013−2022.

(21) Camacho, E. F.; Bordons, C. *Model Predictive Control*; Springer London, 2007; pp 81−125.

(22) Sarath Yadav, E.; Indiran, T. PRBS based model identification and GPC PID control design for MIMO Process. *Mater. Today: Proc.* **2019**, *17*, 16−25.

(23) Kouvaritakis, B.; Cannon, M. *Model Predictive Control*; Springer International Publishing: Switzerland, 2016; pp 1−62.

(24) Åström, K. J.; Hägglund, T. The future of PID control. *Contr. Eng. Pract.* **2001**, *9*, 1163−1175.

(25) Preitl, S.; Precup, R.-E.; Preitl, Z.; Vaivoda, S.; Kilyeni, S.; Tar, J. K. Iterative Feedback and Learning Control. Servo systems applications. *IFAC Proc. Vol.* **2007**, *40*, 16−27.

(26) Vrkalovic, S.; Lunca, E.-C.; Borlea, I.-D. Model-free sliding mode and fuzzy controllers for reverse osmosis desalination plants. *Int. J. Artif. Intell.* **2018**, *16*, 208−222.

(27) Rathore, N. S.; Singh, V. P.; Kumar, B. Controller design for doha water treatment plant using grey wolf optimization. *J. Intell. Fuzzy Syst.* **2018**, *35*, 5329−5336.

(28) Sahu, B. K.; Pati, S.; Mohanty, P. K.; Panda, S. Teaching−learning based optimization algorithm based fuzzy-PID controller for automatic generation control of multi-area power system. *Appl. Soft Comput.* **2015**, *27*, 240−249.

DOI: 10.1021/acsomega.9b02713
ACS Omega 2019, 4, 21230−21241

(29) Seth, S.; Agrawal, Y. C.; Ghosh, P. K.; Jayas, D. S.; Singh, B. P. N. Oil extraction rates of soya bean using isopropyl alcohol as solvent. *Biosyst. Eng.* **2007**, *97*, 209−217.
(30) Ewell, R. H.; Harrison, J. M.; Berg, L. Azeotropic distillation. *Ind. Eng. Chem.* **1944**, *36*, 871−875.
(31) Alves, R. M. B.; Quina, F. H.; Nascimento, C. A. O. New approach for the prediction of azeotropy in binary systems. *Comput. Chem. Eng.* **2003**, *27*, 1755−1759.
(32) Ogunnaike, B. A.; Ray, W. H. *Process Dynamics, Modeling, and Control*; Oxford University Press: New York, 1994; Vol. *1*, pp 1−54.
(33) Skogestad, S. Dynamics and Control of Distillation Columns - A Critical Survey. *Model. Identif. Control* **1997**, *18*, 177−217.
(34) Martin, P. A.; Odloak, D.; Kassab, F. Robust model predictive control of a pilot plant distillation column. *Contr. Eng. Pract.* **2013**, *21*, 231−241.
(35) Mansouri, S. S.; Huusom, J. K.; Gani, R.; Sales-Cruz, M. Systematic integrated process design and control of binary element reactive distillation processes. *AIChE J.* **2016**, *62*, 3137−3154.
(36) Andersen, H. W.; Kümmel, M.; Jørgensen, S. B. Dynamics and identification of a binary distillation column. *Chem. Eng. Sci.* **1989**, *44*, 2571−2581.
(37) Eisinberg, A.; Fedele, G.; Frascino, D. An analytic optimization procedure to estimate a first-order plus time delay model from step response. *2008 16th Mediterranean Conference on Control and Automation*, 2008; pp 729−734.
(38) Fedele, G. A new method to estimate a first-order plus time delay model from step response. *J. Franklin Inst.* **2009**, *346*, 1−9.
(39) Wood, R. K.; Berry, M. W. Terminal composition control of a binary distillation column. *Chem. Eng. Sci.* **1973**, *28*, 1707−1717.
(40) Abu-Ayyad, M.; Dubay, R. MIMO extended predictive control-implementation and robust stability analysis. *ISA Trans.* **2006**, *45*, 545−561.
(41) Yuan, H.-B.; Na, H.-C.; Kim, Y.-B. Robust MPC−PIC force control for an electro-hydraulic servo system with pure compressive elastic load. *Contr. Eng. Pract.* **2018**, *79*, 170−184.
(42) Johnson, M. A.; Moradi, M. H. *PID Control*; Springer, 2005; pp 473−515.
(43) Abdelrauf, A. A.; Abdel-Geliel, M.; Zakzouk, E. Adaptive PID controller based on model predictive control. *2016 European Control Conference (ECC)*, 2016; pp 746−751.
(44) Sato, T.; Inoue, A.; Yamamoto, T. Improvement of tracking performance in designing a GPC-based PID controller using a time-varying proportional gain. *IEEJ Trans. Electr. Electron. Eng.* **2006**, *1*, 438−441.
(45) Shridhar, R.; Cooper, D. J. A tuning strategy for unconstrained SISO model predictive control. *Ind. Eng. Chem. Res.* **1997**, *36*, 729−746.
(46) Abu-Ayyad, M.; Dubay, R.; Kember, G. C. SISO extended predictive control formulation and the basic algorithm. *ISA Trans.* **2006**, *45*, 9−20.
(47) Saeed, Q.; Uddin, V.; Katebi, R. Multivariable predictive PID control for quadruple tank. *World Acad. Sci. Eng. Technol.* **2010**, *4*, 861−866.

DOI: 10.1021/acsomega.9b02713
ACS Omega 2019, 4, 21230−21241